



A Study on the Modified Algorithm for Image Processing in Tracking Seam Welding

Y. Pourasad^a, A. Afkar^b

^a Faculty of Electrical Engineering, Urmia university of Technology, Urmia, Iran

^b Technology and Engineering Research Center, Standard Research Institute, Karaj, Iran

PAPER INFO

Paper history:

Received 10 November 2020

Received in revised form 23 December 2020

Accepted 04 January 2021

Keywords:

Morphological Filter

Welding Robot

Non-destructive Tests

Feature Extraction

Ultrasonic

Least Squares

Image Processing

ABSTRACT

For robot path planning the weld seam positions need to be known in advance as the industrial robots generally work in teach and playback mode. Since the welding of the pipe is not done completely on the straight line (the nature of the pipe) and the test tube under the machine is moving, the symmetry of the two probes in relation to the welding site is very important during the test and quick tracking is required to set the probes. The use of image processing and machine vision techniques is very efficient in optimizing seamless welding radii. In designing the algorithms used, an attempt has been made to reduce the environmental conditions and unstable industrial situation well in order to track the weld seam with an acceptable speed. New approach has been used to access the central line of the weld seam area. The algorithm is designed to be implemented in a real environment and has very good results. One of the advantages of this method is the reduction of measurement error and the elimination of mechanical and electrical sensors in non-destructive tests.

doi: 10.5829/ije.2021.34.08b.13

1. INTRODUCTION

In the area of connecting the welding parts, the edges of the pieces are tangled together and close together to form a weld joint [1-3]. Another notion of welding is the boiling area after the welding operation on the piece. For inspecting imperfections, welding seals are designed to accurately and precisely control the head of the system at the center of the gun, which can be used for welding purposes such as a welding torch and a welding inspection of the head, a test and inspection device probe assembly. Figures 1 and 2 present the weld seam before and welded area after weldings, respectively.

Extensive research was carried out by Xizhang et al. [4], Yong et al. [5] and Xu et al. [6] on seamless welding detector system, which was based on the active method. The use of Laplacian Gaussian function, thresholding using the maximum squared difference method, use of the tagging technique, thin work and

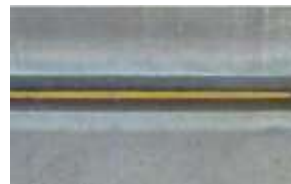


Figure 1. Weld seam before welding



Figure 2. Welded area after welding operation

find skeletons, the extraction of feature regions in this study is first partitioned using the image Laplacian of Gaussian (LoG) filter and the laser profile is extracted, then, to remove the discontinuities, the average filter is used. Continuation of the algorithm is based on the tagging technique. By calculating the meters and considering that the largest meter (label) is the weld profile. The largest label is left with the calculation of the length of the labels, and the remaining labels are deleted. To gain access to the characteristics of the weld profile property, this should be done using a weld profile sketch, the feature points in this way are the corners of the laser profile, which calculates the spatial coordinates of those points, and the center of the profile

Corresponding Author Institutional Email: y.pourasad@uut.ac.ir (Y. Pourasad)

with one geometric relationship is obtained. Another algorithm for detection of edge techniques for image segmentation that was announced by Dhankhar and Sahu [7]. The algorithm also operates on an active basis [8], believes that interpolation and hack conversion and pattern recognition algorithms are very costly and reduce the speed of tracking operations, instead offering a new algorithm. They defined the concept as the second central disagreement, which is expressed as follows:

$$2CD(x)=(f(x3)-f(x1))/2 \tag{1}$$

X1 pixel edge profile before the current pixel and X3 is the next pixel on the laser profile. An algorithm developed by Bender et al. [9] to detect the weld seam at the edges of the wound based on the active method. In this method, he defined the location of the intersection of the laser and the weld seam as this feature point. In fact, the laser beam was perpendicular to the weld seam and reflected in the segment. In the first step, for extracting the ROI region, the seam image (sum of intensities) calculated the weld in a vertical direction (column wise) and with respect to the difference in the intensity of the image on the edges of a region, $[UC-dy UC + dy]$ is defined as a column that $UC = \text{Min}(p(j))$ and $p(j)$ is also the image of the j -th row. Therefore, extracting the laser profile also performed the above operation in a row; then sketching and interpolating the feature points. Figure 3 shows the steps of this algorithm on an image of welding.

Noise reduction and smoothing conducted with middle filter, thresholding, skill and thin work, Huff conversion.

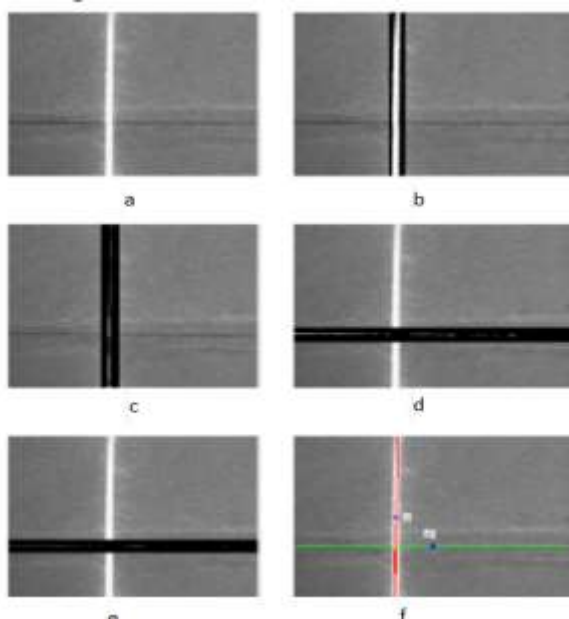


Figure 3. a (initial image), b (ROI region), c (image B), d (f points of the feature), e (Noise reduction), f (f1 and f2 points)

2. METHOD

2. 1. Algorithm Expressed by Tavlin Recently, an algorithm was developed by Bender [9] to detect the welding seam using arc-imaging, similar to the previous methods of its algorithm, including the steps of using the middle filter, manual thresholding, the removal of small areas, the edge detection. Using Robert's algorithm is an interpolation with a quadratic polynomial method, he unlike the previous methods considers seam edges to be two second-order curves.

2. 1. 1. Using Neural Networks and Fuzzy Logic The instability of industrial systems and turmoil in the industrial environment has led many research into the use of neural networks. In many cases, this has improved sustainability and increased reliability of these systems [10-12]. In some studies also, the combination of neural networks and fuzzy logic has been used [13]. But the problems with these methods are the strong dependence of these systems on the design environment, as these systems do not function in other environments, and depend on one special environment.

2. 1. 2. Proposed Algorithm for Seam Welding Detection Due to the problems of the existing vision systems of the existing machine and the use of the active method used in most of the research, our proposed algorithm is based on the method of inactivity, and the hardware and equipment required are also seen, the effects of using inactive method. The complexity of the algorithm is the extraction of the feature and the sensitivity to the removal of environmental conditions. Due to the use of the inactive hardware method in this article and the close relationship between hardware and the machine vision algorithm, the hardware platform of the system is also briefly examined. As shown in Figure 4, the seamless sewage detection system structure consists of several basic components, including: cross-axis, camera (sight sensing), system head (which

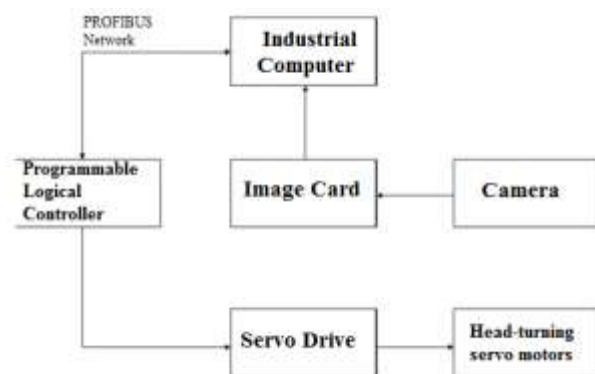


Figure 4. The hardware structure of the seam welding detector to detect the welding seam

includes a tube test tube probe assembly) camera image conversion cards, central controller system, analog-to-digital signal converter cards, head-turning servo motors and an industrial computer.

The crossover axes are controlled by two servomotor 1 controllers. Horizontally controlled motion by the servomotors, along with the control of the welding seam and the precise guidance of the system on the center line of the welding, is carried out by the gearbox to the horizontal axis coupling system, driving the axes in a horizontal direction. The amount of movement and speed of these servomotors depends on the amount of deviation of the system head from the central line, and the goal of the central controller is to minimize this difference so that it can maintain the system head with acceptable error along the center of the system. The mounted motors in the vertical direction also control the height to the pipe surface and vary according to the size of the pipe diameter, which does not need a controller and is manually controlled by the user. The camera sends per second 30 frames from the pipe surface into the computer [14]. In order to increase the reliability of the system for image segmentation and extraction of welder lines, the cutoff technique has been used in two steps, and the edge cutting technique has been used, as well as different edging methods have been evaluated and appropriate mask has been selected. With the characteristics and characteristics of boiling images, different thresholds have been applied to different images. A vertical histogram analysis has also been used for comparative thresholds, the proposed algorithm stages are shown in Figure 5.

2. 1. 3. Sharp Seam Welding Image Smoothing

The use of middle nonlinear filtering is very effective in eliminating random noise as well as pulsed noise, and has less negative effects on the removal of the edges of the weld than linear filters as well as gaseous filters. In order to smoothing and eliminating noise in the proposed algorithm, we used the middle filter, we used

three techniques to eliminate noise in practical studies, the aforementioned techniques are the mean, the mean, and the Gaussian filter. The size of the filter, the smaller the filter is, the less the weld edges disappear and the segmentation accuracy of the image increases. The results of the experiments on different images and the different conditions of welding inspection, the badge; it was mention that the use of the mid-filter is better than the Gaussian filter [15]. It can be said that the average strength of the middle filter is rather resistant to the Gaussian resistance to the momentary changes in intensity in pixels (the amount of pulse intensity is not displayed as a result) as well as the absence of the production of new edges when processing the edges. However, it should be noted that Gaussian filter has a stronger effect in Gaussian noise, unlike the middle filter [16].

2. 2. Detecting the Tube Movement in the Image

In order to increase the speed of the control of the system head and to accurately detect the welding seam, it is necessary to reduce the additional processing and the use of the current image properties. In this way, in extracting successive frames, the current frame difference is used with a new frame, and if a change is made, the new image will be processed. Otherwise, the current system parameters will be changed unchanged to the system head controller as input to the control system.

$$f = \text{median} (f(t + 1) - f(t)) \tag{2}$$

where, f (t) is the image extracted at the moment t, also used to remove possible noise from the middle filter, as well as the second soft value of the resulting image difference with a constant threshold (empirically obtained) compared with the larger image. From a threshold, the new image is processed.

$$\text{motion}(t) = \begin{cases} \text{motion} & \|f\|_2 > T \\ \text{no motion} & \|f\|_2 \leq T \end{cases} \tag{3}$$

$$\|f\|_2 = \sqrt{\sum_{i=1}^n \sum_{j=1}^m |f(x_i, y_j)|^2} \tag{4}$$

A fixed threshold, and motion (t) is a function of image change detection, and the dimensions of the image are n * m; if the square matrix is a second, the second soft matrix is actually the largest singular point of the image matrix, in addition to using the soft two image matrices, we could Use the Accumulative Difference Image method to determine the change in image frames, the ADI matrix is created for a sequence of consecutive frames {f (x, y, t1), f (x, y, t2), ..., f (x, y, tn)}, by comparing each frame with a reference frame count for



Figure 5. Image processing steps in the proposed algorithm

each location. The pixel in the growing image, however, is added where the difference in the pixel location between the reference image and the video frame (of the sequence) occurs. Therefore, when the k frame is compared with the reference frame, the desired value of the ADI indicates the number of times the pixel changes, Equation (5) shows an ADI matrix, which is an absolute ADI type.

$$A_k(x, y) = \begin{cases} A_{k-1}(x, y) + 1, & |R(x, y) - f(x, y, k)| > T \\ A_{k-1}(x, y), & \text{Otherwise} \end{cases} \quad (5)$$

R (x, y) is a reference image, k is the image at time tk, the above relation can be considered as the reference image as the current image, and as long as the ADI layers are no more than a threshold value, this image is considered as a reference, one of the problems of this method The volume of its calculations is high, therefore, we use the first method (soft second of the image difference matrix) in this paper; in none of the previous algorithms of this method (determination of image changes) is not considered, and according to the percentage of low-dimensional changes in consecutive images in some industrial environments, the application of this method can lead to a reduction in the volume of computation in the next steps.

2. 3. Separation of the Seam of the Weld The use of segmentation techniques in the separation of the weld area from the tube body in real conditions can be very difficult. In ideal images, the intensity of the weld regions is greater than the areas around it, but in actual images, the intensity of the images in the two welding regions (starting and finishing areas). Therefore, the choice of a criterion (such as a threshold) is often difficult in the segmentation of welding images. The tests showed that district growth methods and the use of clustering cannot meet our needs, because they are both cost-effective methods and the similarity criterion well, we cannot define it, we discuss the methods in this article that we have used the edges and thresholds, the severe changes on the edges represent the welding seam, and this feature is used to extract the edges.

2. 3. 1. Proposed Method for Weld Seam Segmentation

The results of practical experiments on a seamless weld image showed that the interval of the Sobel algorithm is wider than other algorithms, then the gradient calculations of the image are made to access a suitable seam welding extract using the matrices of Figure 6, given that the welding seam is parallel with the horizon axis, these matrices compute well the horizontal and vertical seams. Gradient image resulting from the application of a twist. 1 Image of a welder is a gray scale image taken from the sum of the two horizontal and vertical components of Figure 7. The resulting image has negative pixels, which

is due to a change in the intensity at the weld septum and the tube body. In these areas, where the intensity of the tube body is less than the intensity of the seam area, the result of applying the matrices is negative, since these areas must be extracted, in this algorithm, the total second power of the pixels is used to reduce the effect of the negative intensity pixels.

2. 4. Segmentation with Cut off Threshold

The resulting gradient image may have noises due to the strengthening of weak edges or unintended edges, one of the problems with the edges obtained is the probability that these edges are real, in other words, the probability of the edges being real To check, the boundary between real and unreal edges should be estimated as a threshold. Several methods have been used for segmentation of images with thresholds. We used this threshold algorithm in two stages of segmentation of images using thresholds. Probability density functions can be used to detect the actual weld seams. In Equation (6), the likelihood of the edge is shown.

$$P_D = \int p(G | \text{edge}) dG \quad (6)$$

where PD is the probability of the realities of the edges, and P (G|edge) is a gradient conditional probability function, provided that the edges are real and t is the

$$\frac{1}{4} \begin{bmatrix} 1 & 0 & -1 \\ 2 & 0 & -2 \\ 1 & 0 & -1 \end{bmatrix} \quad \text{a} \qquad \frac{1}{4} \begin{bmatrix} -1 & -2 & -1 \\ 0 & 0 & 0 \\ 1 & 2 & 1 \end{bmatrix} \quad \text{b}$$

Figure 6. Matrix (mask) horizontal and vertical seam extraction $im=dx^2+dy^2$ where, im gradient image, dx is the vertical component and dy is the vertical component.

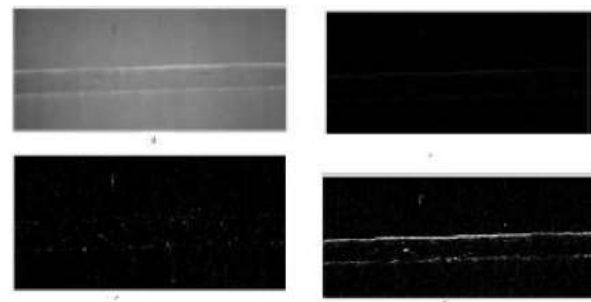


Figure 7. a: Input Image and b: Horizontal Component Image: c: Image of the vertical component; and d: The result of applying the $im = dx^2 + dy^2$

threshold, and the probability of the unrealized and unmerited edges extracted by Equation (7) can be displayed.

$$P_f = \int_1^{\infty} p(G | \text{no-edge}) dG \tag{7}$$

F is the probability of the unreality of the seams, and $P(G | \text{no-edge})$ is the conditional probability of the unreality of the edges. Using the above relations, the probability of the error in the actual welding seam extraction can be written as Equation (8).

$$P_E = (1 - P_D)P(\text{edge}) + (P_f)P(\text{no-edge}) \tag{8}$$

In fact, we can draw the density function as Figure 8 and examine the threshold state.

Selecting a suitable threshold t can be used to reduce the actual PE faces by reducing the actual edges. In fact, if the conditional probability ratio of the real edges is higher than the non-edges; one can hope that a good threshold has been chosen. In other words, if we can establish the relation 10, it can be concluded that the threshold is a useful and appropriate threshold.

$$\frac{p(G + \text{edge})}{p(G | \text{no-edge})} \geq \frac{p(G | \text{no-edge})}{p(G | \text{edge})} \tag{9}$$

The above relations show that the proper threshold selection statistic process requires having information about the probability density and probability functions of the conditional condition of the gradient function, which requires gradient image analysis, which will not be efficient in the real-time system of ours. The parameter shown in the above table is the signal-to-noise ratio defined as follow:.

$$SNR = \left(\frac{h}{\sigma}\right)^2 \tag{10}$$

where, h is the height of the edges of the gradient image and σ is the standard deviation of the image noise, the review of the above table shows that if the noise is low, the SNR of the optimum threshold decreases, as well as in the case of intense noise in the images and low signal

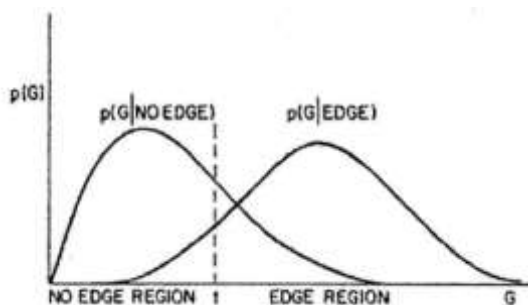


Figure 8. Graph of gradient probability density function

ratio to noise increases the optimum threshold. In addition, as a general rule in cases where $PD = 1 - PF$, in this case the threshold can estimate the signal-to-noise ratio, for example, if $SNR = 100$, the optimal threshold can be approximately 10% of the maximum gradient (William K. Pratt). However, in cases where the signal-to-noise ratio (SNR) is clear in optimum threshold estimates, the SNR parameter calculation is also not easy and costly in most cases, but it can be said that the average normalized gradient image is roughly estimated from SNR and the threshold properly can be an approximation of the root mean square, so you can write the optimal threshold as follows [6].

$$T \cong \sqrt{4 * \text{mean}(fx^2 + fy^2)} \tag{11}$$

By choosing this threshold, they are eliminated as an approximation of the optimal threshold for non-oblique edges. It is more successful in extracting real edges than other images, and very small changes (up to a thousandth) (in the choice of threshold eliminating the real edges or adding a wide range of unreal edges in the binary image. Although, the image obtained from applying an optimum threshold removes a significant portion of the non-edged edges, still has edges and unnecessary noise, which is due to the choice of a threshold instead of several thresholds and should be removed with further methods.

3. RESULTS

3. 1. Histogram Analysis

The choice of the appropriate threshold for separating the weld from the tube body is a key step in seamless tracking. After segmentation by cutting the edge, thresholding for the final seam cut is used, but as mentioned in some images still have many unobtrusive edges that should be removed, histogram analysis, and the use of variance. Atoso method has been used in many seam welding tracking methods [12]. In the practical test, the above methods did not succeed in weld images of all of the above methods, and practically eliminated a large part of the useful edges or created many unnecessary edges that, in the process of processing the extraction algorithm, faced the characteristics with a fundamental problem, one of the factors of the failure of the above methods is due to this feature that the difference in intensity between the seam and the bottom of the tube is not very high and the histogram of the images does not have distinct peaks and in spite of the uncertainty of the correctness of the operation of the above algorithms in the correct segmentation of all the image. The methods rely on repetition, which are very costly, for these reasons, we have to look for a new method for the proper placement of the seamless images.

3. 1. 1. The Proposed Threshold Method

Due to seamless welding images, which is almost parallel to the horizontal axis, this feature can be used to calculate the total intensity of the pixels along horizons (horizontal histogram) along the horizontal axis, so the histogram of each pixel. The row is computed, equation 12 defines the definition of the horizontal histogram (histogram projection). By this definition, for each row, *i* represents the total number of pixels in that row, which is equal to one (binary image) to that row.

$$hist(i) = \sum_{j=1}^M d(xi, yi), P(A) = \sum_{k=1}^N his(k) \tag{12}$$

A is a binary image of N*M dimension, N is the image length of the pixel unit, and M is the image width of the pixel unit. By checking the histogram obtained from equation 14 in different welding images, it was found that this histogram has two different peaks with suitable intervals. Observation, the accumulation of pixels in the weld seams will be higher, and these are the same pixels of seamless welding, so the pixels of our areas around the histogram peaks where the pixels are more focused. Therefore, if you can reconstruct the image by separating these pixels and eliminating the intensity of other pixels away from the peaks, then a successful segmentation has taken place. It is noteworthy to reach a number to estimate the margins of these peaks, by performing numerous experiments on practical images, we conclude that the use of peak (max) (histogram) and applying a coefficient can improve fractional percentages, so the desired threshold relationship that we define it as equation 13.

$$T=a.Max(P(A)) \tag{13}$$

where, a is a coefficient and P(A) is a histogram of the binary image A, which is a coefficient of a to adapt to a very flexible environment. A sample image with histogram and segmental image is shown in Figure 9.

3. 2. Investigating the Algorithm

In dealing with the type of welding, the surface of the pipes in practice there are two basic types of problems that must be considered as a solution for it. Distribution of pixels at two-edged points due to the accumulation of points in

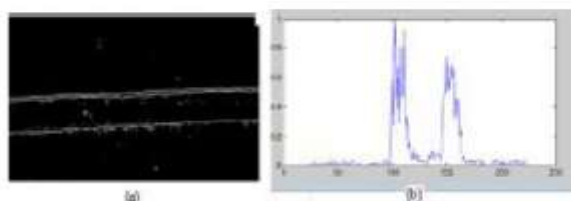


Figure 9. A: A binary image of the welding seam, a: a sectioned image with the proposed method, b: Histogram image

the edges: ruggedness of the welded area. Investigation of welding images in practical tests shows that the disturbances due to the lack of proper welding and the fluctuations of the welding parameters cause the damaged and deformed areas of the weld at the pipe level. Therefore, the extraction of the characteristic in this type of pouring is encountered with difficulty and if there is no proper welding surface, many boundaries, whether real or unrealistic, are created and this creates sharp changes in the histogram of the image, which makes it difficult to detect the maximum points, so the algorithm must be able to correctly and in a user-friendly environment to trace all of these poorly-formed welds.

In Figure 10, the purple spot is the center of the system, calibrated at the beginning of the test, and the point is red in the center of the weld seams, and *dr* is the distance between these two points.

3. 3. Automatic Ultrasonic Testing

This machine consists of three sections of pipe transfer, seam welding detection and monitoring system at the time of tube testing. The central controller includes the PLC of the Siemens S7 model, and the motor controllers and local sensors are connected to the profibus network to the CPU. The position of the pipe is connected to the plunger connected to the motor by the anchor and controlled by the speed and location of the pipe for the up and down of the ultrasonic levels. The advanced monitoring system provides real-time monitoring and monitoring of ultrasonic signals through profibus and opc communications, providing a data bank for data storage. The transfer of the pipe from the inlet to the outlet and follow the welding seam to detect the ultrasonic probes, as well as the automatic monitoring of the system. To simulate the positioning of two probes in relation to the welding site during the test of a seamless sewage detector system, which is based on image processing techniques and machine-design techniques used in this system. This test consists of two subsections: the tube transfer part and the computer-based monitoring part as shown in Figures 11 and 12, respectively.

3. 3. Evaluation of the Accuracy of the Algorithm (Implementation Method)

In evaluating the accuracy of the system, the amount of deviation from



Figure 10. Position of the center of the seam and the head of the system

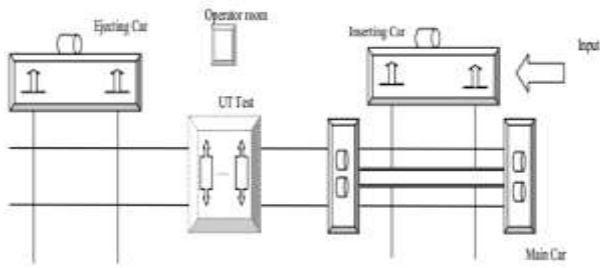


Figure 11. General diagram of pipe transfer



Figure 12. Monitoring system

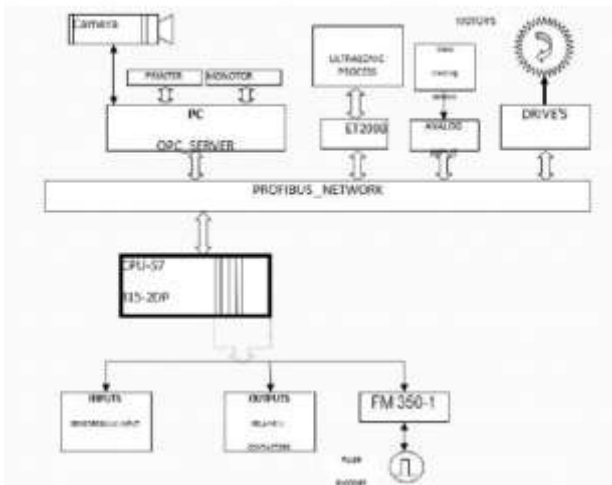


Figure 13. General structure of the automation system of the proposed ultrasonic testing machine

the center of the weld is considered from the center point of the device. The results of this test are presented in Table 1. In order to achieve these results, the system is implemented in a laboratory, and with the installation of hardware and software, the tracking operation. In order to calculate the amount of leakage deviation from the center of the system, a point-of-contact laser source was introduced into the coupler system, which is beamed to the welding seam at the output of the

machine, along with the deviation of the seams. This luminous point also diverged, at the same time, from the surface of the films, the deviation from the centerline was calculated by measuring the amount of distortion in the obtained frames. Considering that the algorithm is designed to extract the two edges of the weld seam, in the two windows execute the seamless pixel thinning operations. Therefore, the final accuracy depends on the accuracy of the algorithm in welding seam welding on both sides. In order to access the criteria for comparing the accuracy of the system, several different images at different intervals from the pipe surface and in different environmental conditions. It was tested with different contrast and resolution, resulting in a seamless deviation. By the proposed algorithm, the actual seam is calculated. According to Equation (13), the system error can be written as Equation (14).

$$d_r \leq 0.5(d_{low} + d_{hi})$$

$$\bar{e} = (\sum_{i=1}^N |e|) / N, i = 1, 2, \dots, N \tag{14}$$

e: The mean error of the system is calculated from Equation (27), if the magnitude of the relation is neglected, the mean of the arithmetic is obtained.

d r: The error rate of the center point of the weld seam is calculated from the actual center of the welding seam.

d low: The low seam extraction error is due to the boiling point of the lower seam.

d hi: The magnitude of the extracted extraction seams exceeds the actual boiling point of the seams.

Of course, due to different sources of error, computational errors and rounding errors of numbers are ignored.

3. 4. Calibration Operations

The precision and accuracy of the results of the algorithm in the industrial environment. In addition to the specific environmental conditions, depends on the visual distance of the machine as well as its viewing angle from the surface of the piece, the more the distance between the sensor (CCD) is less than the surface of the tube; the accuracy of the sampling operation increases in practice. Also, the angle of view of the sensor in the geometric coordinates of the image has a great impact. In the real world, the real coordinates of objects must conform to their coordinates in the image; in practice, there are usually angles between the Cartesian coordinates and in systems that are used for measurement. The relationships between the axes of the coordinates in the image and their actual axes in the environment must be calculated. In this, research we have set the angle between the axes of the coordinates in the image and the real coordinates of the system and set the sensor perpendicular to the direction of the tube movement. So that the axes are inconsistent and the only parameter to be calculated is the scale factor.

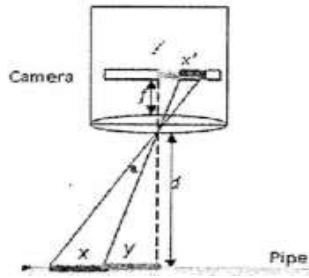


Figure 14. Connection between the camera and its distance from the pipe surface

$$\frac{x}{x'} = \frac{d}{f} \tag{15}$$

where, f is the focal length of the sensor lens and d is the distance between the camera and the tube and x is the part of the image and x' is the image of this section in the sensor x, f, d in length unit (mm), x picture size in the real world is the need to know the resolution of the pixel to calculate it.

$$x' = h(\text{count}(\text{pixel})) \tag{16}$$

where, h is the pixel factor. To calculate, h we use a standard ruler and, at a specified distance, by imaging a sample tube (pipe pipe), which is created in accordance with the standard pipe production, a pipe, and throughout the project that the calibration of different devices is used and the relationship (5) to determine the value of h .

$$s' = \text{pixel count for } S; \quad s = 10\text{mm}, \quad \frac{s}{s'} = h \tag{17}$$

In Table 1, in the first column, the value of h is calculated for different images at different intervals, depending on equation 3. The image size in the visual sensor is related to the distance from the image of the image. Therefore, at different intervals, different numbers for h is obtained. In Tables 1 and 2, the result of the algorithm's execution on fifty different frames shows the test of a pipe after calibration, in this $d_{r,low}, d_{hi}, h = 0.168\text{mm} / \text{pixel}$ test. The point in examining the results of the tables is that since the weld seam center error is computed, in most cases, the final error of the seam welding center has decreased, which increases the accuracy of the algorithm.

Given that the direction of movement along the y -axis is evaluated, only the spatial coordinates of this direction are evaluated; in Figure 16, on the number of frames of an analytical tube, the center of the welding seam in each frame is calculated by the proposed algorithm. The error rate is also measured from the actual boiling point. In section (a), this difference is in millimeters, and in (b) the difference is in pixels, since

TABLE 1. Sampling from the result of the algorithm implementation on fifty frames of the test of a pipe (I)

No.	d_{hi} (pixel)	d_{low} (pixel)	d_r (pixel)	d_r (mm)
P5	3	3	3	0.504
P10	-1	2	1	0.168
P15	1	-4	-2	-0.336
P20	-3	1	-2	-0.336
P25	-2	-6	-4	-0.672

TABLE 2. The result of the algorithm implementation on fifty frames of the test of a pipe (Part II)

No.	d_{hi} (pixel)	d_{low} (pixel)	d_r (pixel)	d_r (mm)
P5	-2	2	-4	-0.672
P10	-3	2	-1	0.168
P15	2	3	2	0.336
P20	4	2	3	0.504
P25	1	3	1	0.168

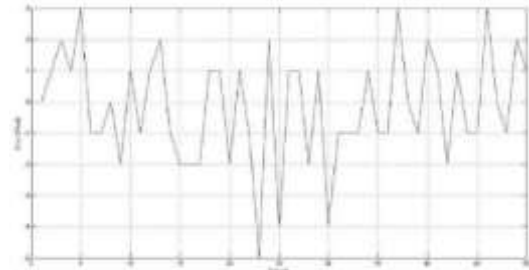


Figure 15. Tolerance diagram (deviation) of weld seam center calculated by the proposed algorithm from the actual center of weld seam in pixels

the deviation from the center is dependent on the value of h ($h = 0.168\text{mm} / \text{pixel}$) the accuracy of the algorithm is also based on the number of pixel deviation per millimeter.

$$\begin{aligned} \bar{x} &= 1.5 \text{ pixel} = 1.5 * 0.168 = 0.252 \text{ mm} \\ \bar{E} &= -0.2 \text{ pixel} = -0.2 * 0.168 = 0.0336 \text{ mm} \\ \sigma &= 1/50 \sqrt{\sum_{i=1}^{50} (|x_i| - 1.5)^2} = 6.4807 \text{ pixel} \end{aligned} \tag{18}$$

4. CONCLUSION

In the field of machine vision in nondestructive welding, there are many things that can be the basis for future research, these can be very effective in improving the efficiency of existing algorithms, such as the following.

- The use of multilayer neural networks for machine training in the estimation of the weld seam at the pipe inspection. It should be noted that neural network research in the welding section has been performed on the calculation of the welding arc, however, much research can be pursued in the area of welding inspection.
- Using fuzzy controllers to design a seam welding detection controller using fuzzy logic ++ software and Siemens systematic software.
- Development and design of integral and derivative controllers to improve the accuracy and speed of seam welding center detection.
- Designing algorithms for detecting non-parallel welds with the axis of motion of the welding machine.
- Development of techniques for eliminating all kinds of actual noise in industrial environments.
- Designing algorithms to draw a three dimensional polygonal pattern (pool welding) for more accurate tracing of the weld seam.
- Development of segmentation techniques for identifying the typical welds type of welds activated in weld inspection.
- Designing algorithms for tracking asymmetric welds.
- Using Kalman's algorithm (Kalman Filter) to detect and track the seam welding center.
- Providing combined methods for improving the mineral method and Atos method in welding seam extraction.
- Evaluating the effectiveness of methods such as active contour.

5. REFERENCES

1. Fang, Z.J. and Xu, D., "Application of vision sensor to seam tracking of butt joint in container manufacture", *Embedded Visual System and Its Applications on Robots*, (2010), 56-82.
2. Fang, Z., Xu, D. and Tan, M., "Visual seam tracking system for butt weld of thin plate", *The International Journal of Advanced Manufacturing Technology*, Vol. 49, No. 5, (2010), 519-526, doi: 10.1007/s00170-009-2421-0.
3. Gao, X., Ding, D., Bai, T. and Katayama, S., "Weld-pool image centroid algorithm for seam-tracking vision model in arc-welding process", *IET Image Processing*, Vol. 5, No. 5, (2011), 410-419, doi: 10.1049/iet-ipr.2009.0231.
4. Chen, X., Chen, S., Lin, T. and Lei, Y., "Practical method to locate the initial weld position using visual technology", *The International Journal of Advanced Manufacturing Technology*, Vol. 30, No. 7, (2006), 663-668, doi: 10.1007/s00170-005-0104-z.
5. Wu, Y.Q., Yuan, Z.H. and Wang, J.H., "A fuzzy controller design of seam tracking for welding robot", in *Advanced Materials Research, Trans Tech Publ.* Vol. 442, (2012), 370-374.
6. Xu, P., Xu, G., Tang, X. and Yao, S., "A visual seam tracking system for robotic arc welding", *The International Journal of Advanced Manufacturing Technology*, Vol. 37, No. 1-2, (2008), 70-75, doi: 10.1007/s00170-007-0939-6.
7. Dhankhar, P. and Sahu, N., "A review and research of edge detection techniques for image segmentation", *International Journal of Computer Science and Mobile Computing*, Vol. 2, No. 7, (2013), 86-92.
8. Fattahzadeh, M. and Saghaei, A., "A statistical method for sequential images-based process monitoring", *International Journal of Engineering*, Vol. 33, No. 7, (2020), 1285-1292.
9. Bender, G. and Simonsen, R.R., "Photography's materialities: Transatlantic photographic practices over the long nineteenth century, Leuven University Press, (2021).
10. Devanathan, R., Chan, S.P. and Chen, X., Techniques of automatic weld seam tracking, in *Advanced automation techniques in adaptive material processing*. 2002, World Scientific.125-166.
11. Kheradmandan, H. and Barati, F., "Modeling width of weld in saw with adding nano material", *Journal of Research in Science, Engineering and Technology*, Vol. 5, No. 02, (2017), 1-7.
12. Mashadi, B., Mahmoodi-K, M., Kakaee, A.H. and Hosseini, R., "Vehicle path following control in the presence of driver inputs", *Proceedings of the Institution of Mechanical Engineers, Part K: Journal of Multi-body Dynamics*, Vol. 227, No. 2, (2013), 115-132, doi: 10.1177/1464419312469755.
13. Fakoor, M., Kosari, A. and Jafarzadeh, M., "Humanoid robot path planning with fuzzy markov decision processes", *Journal of Applied Research and Technology*, Vol. 14, No. 5, (2016), 300-310, doi.
14. Meyghani, B., Awang, M. and Wu, C., "Thermal analysis of friction stir welding with a complex curved welding seam", *International Journal of Engineering, Transactions A: Basics*, Vol. 32, No. 10, (2019), 1480-1484, doi: 10.5829/ije.2019.32.10a.17.
15. Salehpour, F., Nematifard, V., Maram, G. and Afkar, A., "Experimental investigation of tig welding input parameters effects on mechanical characteristics", *International Journal of Engineering, Transactions B: Applications*, Vol. 34, No. 2, (2021), 564-571, doi: 10.5829/ije.2021.34.02b.30.
16. Xue, B., Chang, B., Peng, G., Gao, Y., Tian, Z., Du, D. and Wang, G., "A vision based detection method for narrow butt joints and a robotic seam tracking system", *Sensors*, Vol. 19, No. 5, (2019), 1144, doi: 10.3390/s19051144.

Persian Abstract

چکیده

برای برنامه ریزی مسیر ربات ، موقعیت درز جوش باید از قبل شناخته شود زیرا ربات های صنعتی معمولاً در حالت آموزش و پخش کار می کنند. از آنجا که جوشکاری لوله به طور کامل بر روی خط مستقیم (ماهیت لوله) انجام نمی شود و لوله آزمایش در زیر دستگاه در حال حرکت است ، تقارن دو پروب نسبت به محل جوشکاری در هنگام آزمایش بسیار مهم است و برای تنظیم کاوشگرها ردیابی سریع لازم است. استفاده از تکنیک های پردازش تصویر و بینایی ماشین در بهینه سازی شعاع جوشکاری بدون درز بسیار کارآمد است. در طراحی الگوریتم های مورد استفاده ، سعی شده است شرایط محیطی و وضعیت ناپایدار صنعتی به خوبی کاهش یابد تا درز جوش با سرعت قابل قبول ردیابی شود. روش جدیدی برای دسترسی به خط مرکزی ناحیه درز جوش استفاده شده است. الگوریتم طراحی شده است تا در یک محیط واقعی اجرا شود و نتایج بسیار خوبی دارد. یکی از مزایای این روش کاهش خطای اندازه گیری و حذف حسگرهای مکانیکی و الکتریکی در آزمایش های غیرمخرب است.
